

## **Supplemental Material to:**

**Judith Reeks, Shirley Graham, Linzi Anderson,  
Huanting Liu, Malcolm F. White and James H. Naismith**

**Structure of the archaeal Cascade subunit Csa5:  
Relating the small subunits of CRISPR effector complexes**

**2013; 10(5)**

**<http://dx.doi.org/10.4161/rna.23854>**

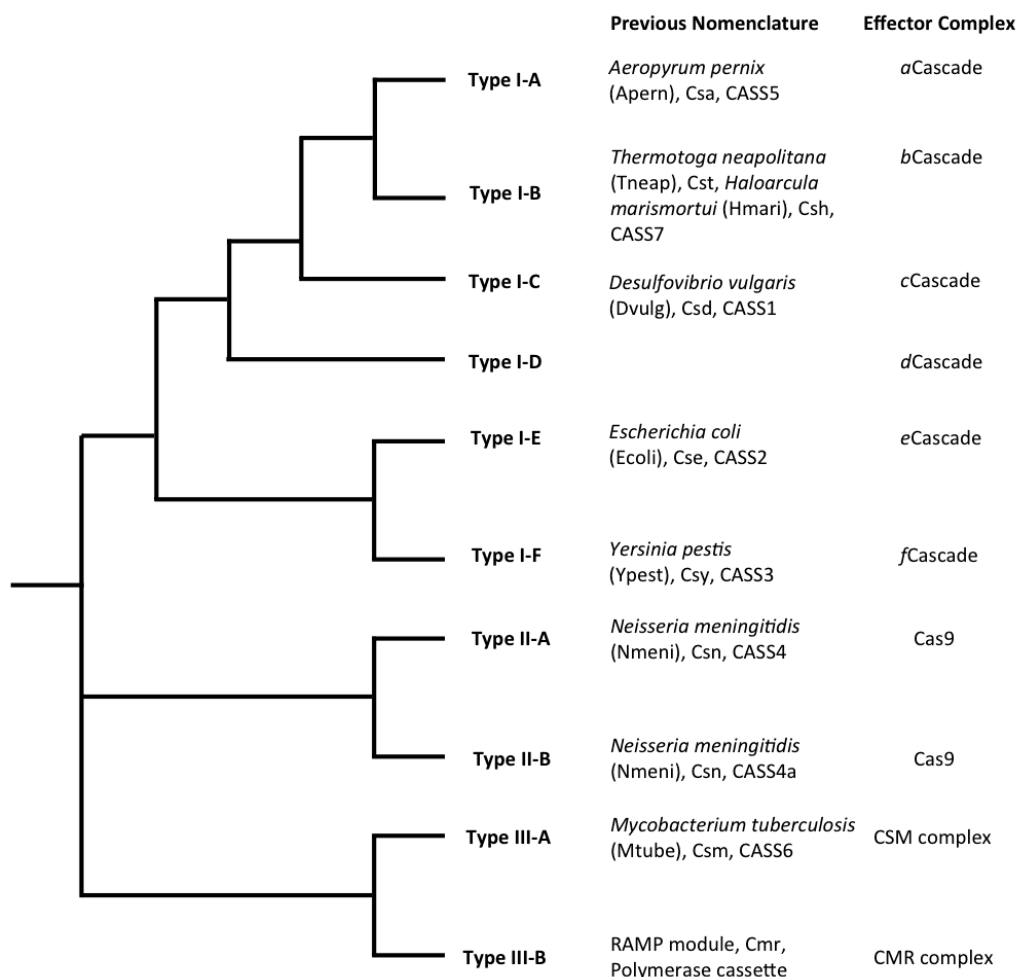
**<http://www.landesbioscience.com/journals/rna/article/23854>**

Oligonucleotide	Sequence
crRNA	5'-FAM-AUUGAAAGACCAUACCCAACUUCUAACAACGUCGUUCU AACAACGGAUUAAUCCAAAA
Protospacer	5'-GATCCTCTCCACGTTGTTAAGAACGACGTTGTTAGAAGTTGGGT ATGGTTGGCTG
Non-target	5'-FAM-CCTCGAGGGATCCGTCCTAGCAAGCCGCTGCTACCGGAA
ssDNA	GCTTCTGGACC

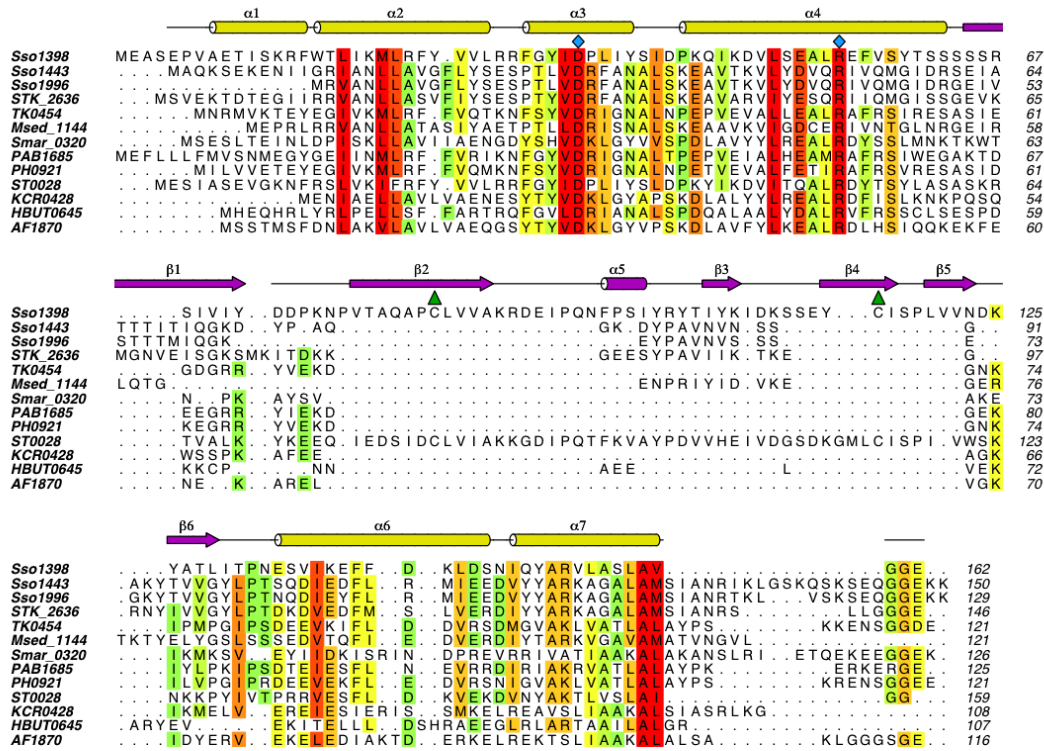
### **Supplementary Table**

**Supplementary Table 1.** Sequences of synthetic oligonucleotides used during fluorescence anisotropy experiments. The spacer, protospacer and PAM sequences are highlighted. 6-carboxyfluorescein (FAM) modifications are indicated.

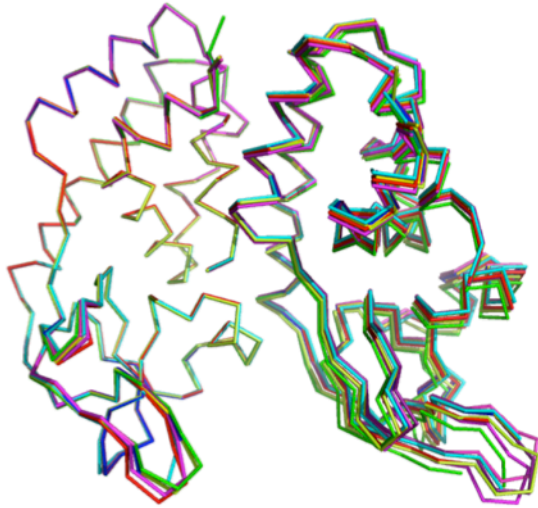
## Supplementary Figures



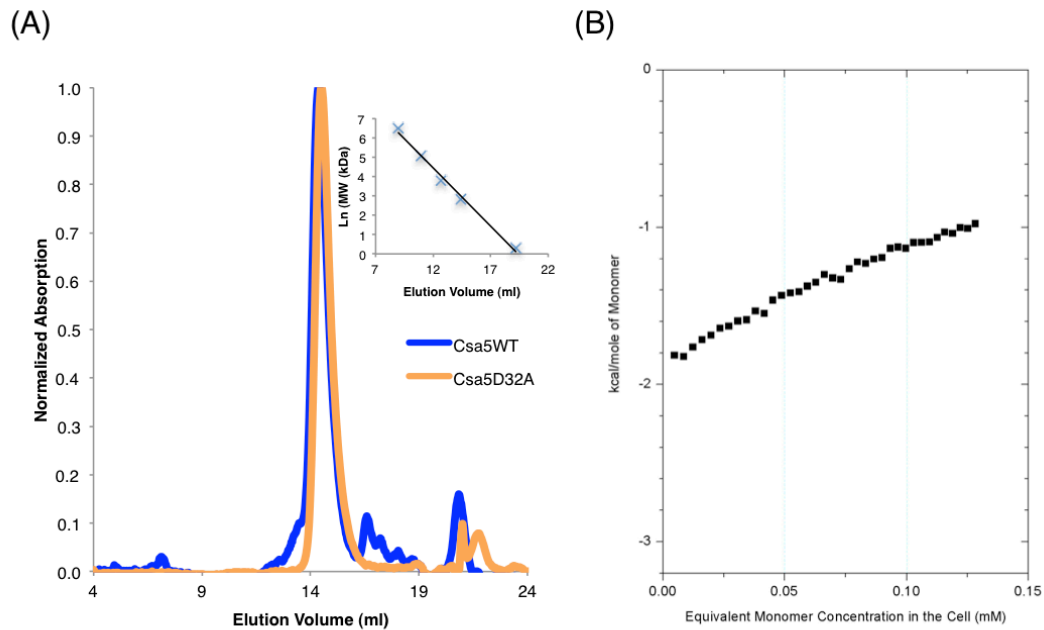
**Supplementary Figure 1.** The current nomenclature for the CRISPR/Cas systems based on the classification described by Makarova *et al.*<sup>10</sup> Previous nomenclature from Haft *et al.*<sup>9</sup> and Makarova *et al.*,<sup>42</sup> which is still widely used in the literature, is shown. Type I-D is newly recognized as a distinct subtype and so has no previous nomenclature. The names of the interference effector complexes are also shown.



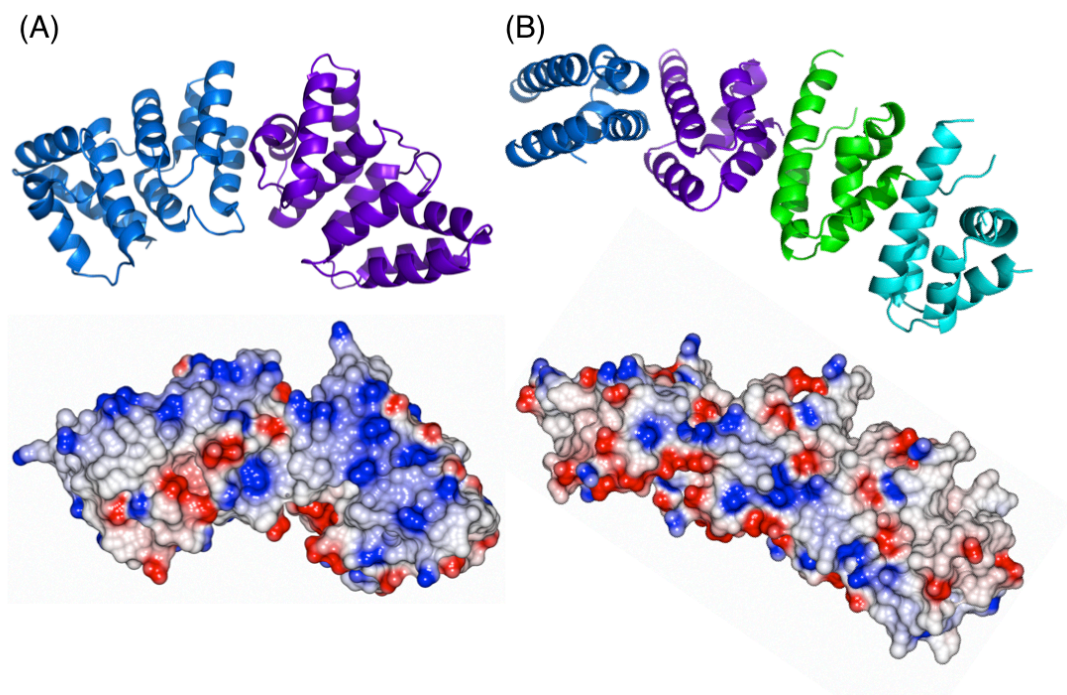
**Supplementary Figure 2.** Sequence alignment of Csa5 proteins. The secondary structure of Sso1398 is shown above the alignment in yellow ( $\alpha$ -domain) and purple ( $\beta$ -domain). The conserved Asp35/Arg55 salt bridge is marked with blue diamonds and the non-conserved Cys85/Cys116 disulfide bridge with green triangles. The alignment was performed using ClustalW<sup>43</sup> and then manually edited. The figure was created using Aline.<sup>44</sup> [ENREF\\_38](#)



**Supplementary Figure 3.** Analysis of the monomer-monomer interfaces in the crystal structure of Sso1398 by superimposing the nine dimer pairs on each other using the first monomer (left). This shows that the interface exhibits a level of plasticity.

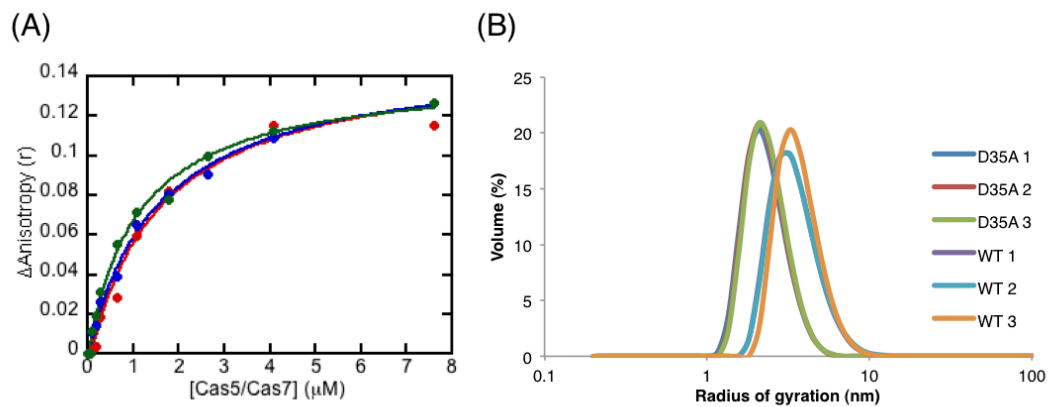


**Supplementary Figure 4.** Analysis of the effect of the Csa5D32A mutation. (A) Gel filtration elution profiles showing that Csa5D32A elutes as a monomer (expected 17 kDa, observed 19 kDa). The calibration curve is shown in the panel. (B) ITC experiment showing that Csa5D32A does not show a significant heat of dissociation upon dilution, which confirms a monomeric species. ITC experiments were performed using a VP-ITC microcalorimeter (MicroCal) at 20 °C using a buffer of PBS with 250 mM NaCl. 540  $\mu$ M Csa5D32A was injected into buffer in 37 x 7.5  $\mu$ l aliquots. The data were analysed in Origin (OriginLab).



**Supplementary Figure 5.** Comparison of the TthCse2 dimer and a homology model of a Csa5 tetramer. (A) The TthCse2 dimer structure (top) and electrostatic surface potential (bottom) clearly showing the positively charged face of the dimer. (B) Homology model of the Csa5  $\alpha$ -domain arranged as a tetramer based on the Sso1398 method of oligomerization (top) and the electrostatic surface potential (bottom). A narrow cleft of positive charge is located across the oligomer. The homology model was created using SWISS-MODEL using the Sso1398  $\alpha$ -domain.<sup>45</sup>

<sup>46</sup> Electrostatic surface potentials were calculated using CCP4MG.<sup>41</sup>



**Supplementary Figure 6 (for reviewers only).** Further data is provided for the reviewers to show that the data presented is representative of all the data collected. (A) The three fluorescence anisotropy traces used for the averaged trace in Fig. 2A are shown. The traces are not significantly different. (B) The DLS measurements were performed in triplicate but only a single representative trace was presented in Fig. 4B. None of the traces vary significantly from each other.